# " COMMISSIONING AND CHARACTERIZATION OF THE MANITOBA AUTOMATED HIGH ENERGY PROTON MICROPROBE, AND THE ROLE OF COLD AND HOT FUSION IN THE IMPLANTATION OF PALLADIUM AND INDIUM BY DEUTERONS"

BY

YOU HUAN YEO

A THESIS

Submitted to the Faculty of Graduate Studies in Partial
Fulfilment of the Requirements for the Degree of

MASTER OF SCIENCE

Department of Physics
University of Manitoba
Winnipeg, Manitoba

OCT 1989

National Library
of Canada

Bibliothèque nationale
du Canada

Canadian Theses Service

Service des thèses canadiennes

Ottawa, Canada
K1A 0N4

ISBN 0-315-54938-6

# COMMISSIONING AND CHARACTERIZATION OF THE MANITOBA AUTOMATED HIGH ENERGY PROTON MICROPROBE, AND THE ROLE OF COLD AND HOT FUSION IN THE IMPLANTATION OF PALLADIUM AND INDIUM BY DEUTERONS

BY

YOU HUAN YEO

A thesis submitted to the Faculty of Graduate Studies of
the University of Manitoba in partial fulfillment of the requirements
of the degree of

MASTER OF SCIENCE

# Abstract

A high energy proton microprobe has been constructed on a dedicated beamline at the University of Manitoba Accelerator Centre. Chapter one describes the extensive program of design and development of the major components of the microprobe. These developments include the design of the target chamber, the object slit and the beam scanning stage. The performance of the major components and the overall system to date is assessed.

Chapter two describes the experiment involving the implantation of deuterons into the palladium and indium targets. This experiment was designed to observed the possible neutrons resulting from the so-called 'cold fusion' effect when there is a sufficiently high concentration of deuterium nuclei present in the target samples. The motivation was to simulate the Utah electrolysis experiment in a non-equilibrium situation not involving heavy water as the intermediate material. A significant neutron production was observed in the implantation experiment and a preliminary examination on the role of 'cold' and 'hot' fusion in this experiment is described.

# Acknowledgements

The author wishes to express his gratitude to Dr. J.S.C. McKee for his effective supervision, guidance and unfailing support throughout the course of these research works.

It is a pleasure to thank Dr. M.S. Mathur, Dr. G.R. Smith and Mr. J.J.G. Durocher who have contributed a great deal of advice and practical help without which these projects would not have been brought to a conclusion.

The help and advice from Mr. K.M. Furutani and Mr. J.K. Mayer are greatly appreciated.

Thanks are also due to members of the University of Manitoba Accelerator Centre support staff and Mechanical and Electrical workshop personnel of the Department of Physics for their advice and help during various stages of the research work.

## Table of Contents

Page

Chapter Two: The Role of Cold and Hot Fusion in the Implantation of Palladium and Indium by Deuterons. 33

# Chapter One

## Commissioning and Characterization of the Manitoba Automated High Energy Proton Microprobe

## 1.1 Introduction

A proton microprobe is an instrument used for the microanalysis of a sample in which a beam of protons is focussed onto a target area of micrometer dimensions. As of 1988, some fifty proton microprobe facilities had been developed [1]. This list includes a new and unique device, the Manitoba Automated High Energy Microprobe (MA-HEM) which has recently been completed at the University of Manitoba Accelerator Centre. It uses the spiral ridge cyclotron as the particle source. The Manitoba high energy microprobe operates at a proton energy of 40 MeV and yields a beam spot approximately 10 μm in diameter. This microprobe is designed to exploit features not available to microprobes operating at a few MeV incident proton energy. Because 40 MeV protons have a considerably larger range in matter and a lower energy loss as compared to low energy protons (1-5 MeV), MA-HEM is an ideal instrument for thin sample transmission microanalysis. Also at 40 MeV, the yield for K x-ray production is at or near its maximum value for most rare earth and medium to large Z heavy elements [2,3]. MA-HEM can measure elemental concentrations at the 1 ppm level for all elements from arsenic to uranium in the periodic table. This level is a factor of 100 times lower than that obtained by low energy proton microprobes and 1000 times lower than that reached by scanning electron microscopes.

When used in conjunction with the proton induced x-ray emission (PIXE) technique, MA-HEM becomes a microscope able to examine the details of elemental composition of geological samples at the inclusion level, biological samples at the cellular level and physical samples at the micron level.

## 1.2 Description of MA-HEM Assembly

The schematic layout for MA-HEM is shown in Figure 1.2.1. The 40 MeV proton beam leaves the cyclotron through a slit of dimensions 5 mm x 12 mm in the x- and y- directions respectively. The direction of propagation of the beam is along the z-axis. It is first focussed by a preconditioning magnetic quadrupole doublet ($Q_a$, $Q_b$) to produce an image at the 70 μm x 70 μm microprobe object slit, 5.49 m downstream from the cyclotron exit slit. Each of the preconditioning quadrupoles has a half aperture of 5.27 cm and an effective length of 31.1 cm. Tne first quadrupole defocusses the beam in the x-z plane and focusses it in the y-z plane. The second quadrupole focusses the beam in the x-z plane and defocusses it in the y-z plane. The operating conditions for $Q_a$ and $Q_b$ are 276 mT and 278 mT respectively.

Another system of four magnetic quadrupoles ($Q_1$, $Q_2$, $Q_3$, $Q_4$), is placed 1.8 m further downstream from the microprobe object collimation slit. Each of the four quadrupoles has an aperture diameter, pole tip to pole tip, of 5.08 cm and an effective length of 21.15 cm. Neighbouring quadrupole magnets are separated by 8 cm. The first and fourth quadrupoles (outer doublet) have equal but opposite fields, as have the second and third doublet (inner doublet). The inner doublet is oriented at 90° relative to the outer doublet. The pole tip magnetic field for the inner doublet is 599 mT, and 286 mT for the outer doublet. This CDCD[1] (in x-z plane), or DCDC (in y-z plane) configuration, is commonly referred to as a 'Russian quadruplet' [4]. This set of quadrupoles will then focus the proton beam emerging from the object collimation slit to an image spot 10 μm in diameter at a distance of 20 cm from the exit of the fourth magnet of the quadruplet system. A beam current at the sample of 300 pA per μA extracted from the accelerator, is measured by means of a secondary electron emission monitor placed 0.5 m from the focus of the microprobe.

---

[1] C: Converging, D: Diverging

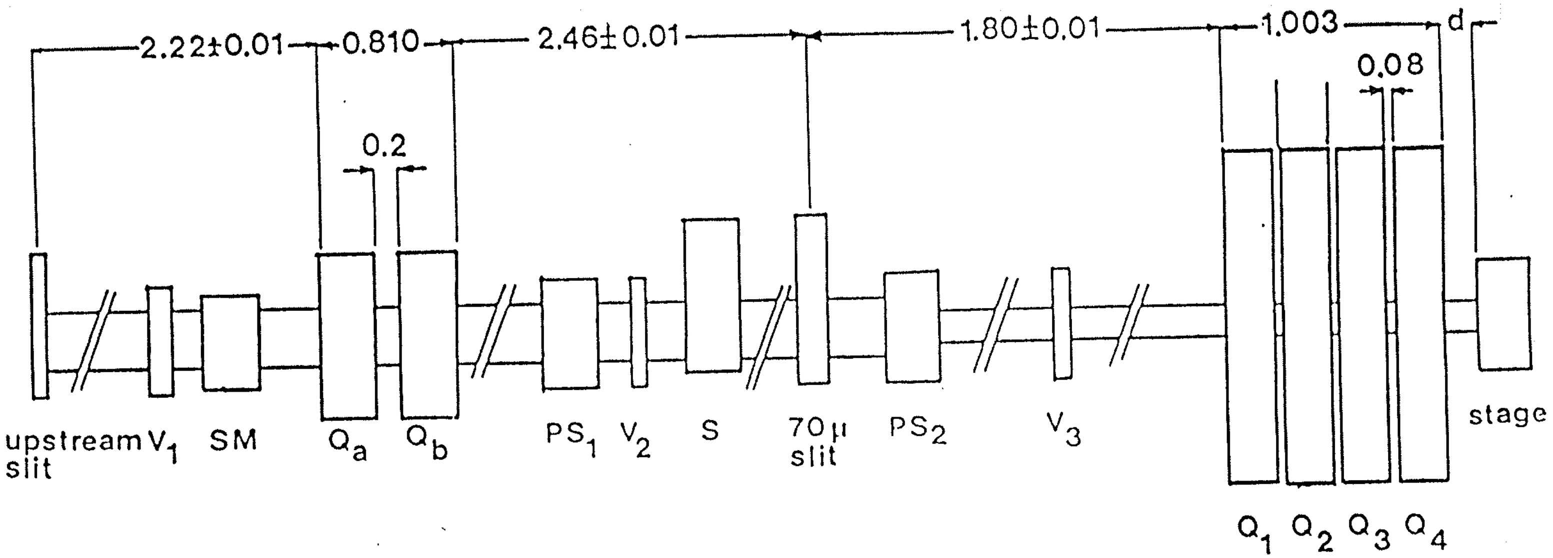

Figure 1.2.1 Schematic layout of the MA-HEM assembly. $V_1$,$V_2$ and $V_3$ are vacuum valves, $PS_1$ and $PS_2$ are pumping stations, S is the viewing screen and the final image point is at a distance d=0.20 m behind the limits of $Q_4$.

## 1.3 Optimization and Alignment

### 1.3.1 The Object Slit

The object slits of a microbeam system are crucial to the attainment of small spot size. The MA-HEM Object collimation slits were constructed from stainless steel. This collimator design incorporates two crossed slits with entrance and exit angles of $15^{\circ}$ and $2^{\circ}$ respectively [5]. The slit design is shown schematically in Figure 1.3.1, where R represents the proton range in steel. The entrance and exit angles are also indicated.

A laser diffraction technique was used to calibrate the MA-HEM object slit. The experimental set-up is shown in Figure 1.3.2. A He-Ne laser with wavelength 632.8 nm was used. By observing the interference pattern on the screen which resulted from a laser beam incident on the object slit, the dimensions of the slit are calculated using the following equations [6],

$$a=(m+1/2)\lambda r/x$$

$$b=(n+1/2)\lambda r/y$$

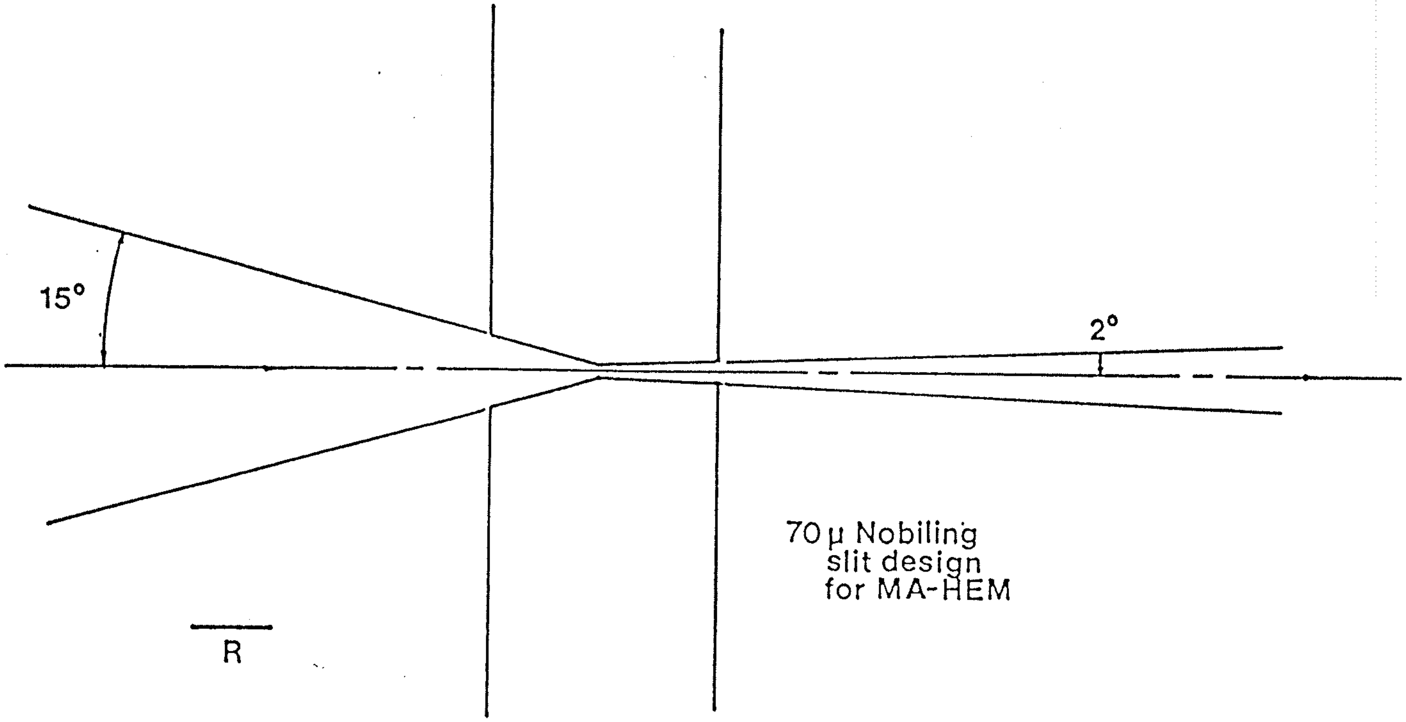

Figure 1.3.1 The MA-HEM object slit, where R is the proton range in steel.

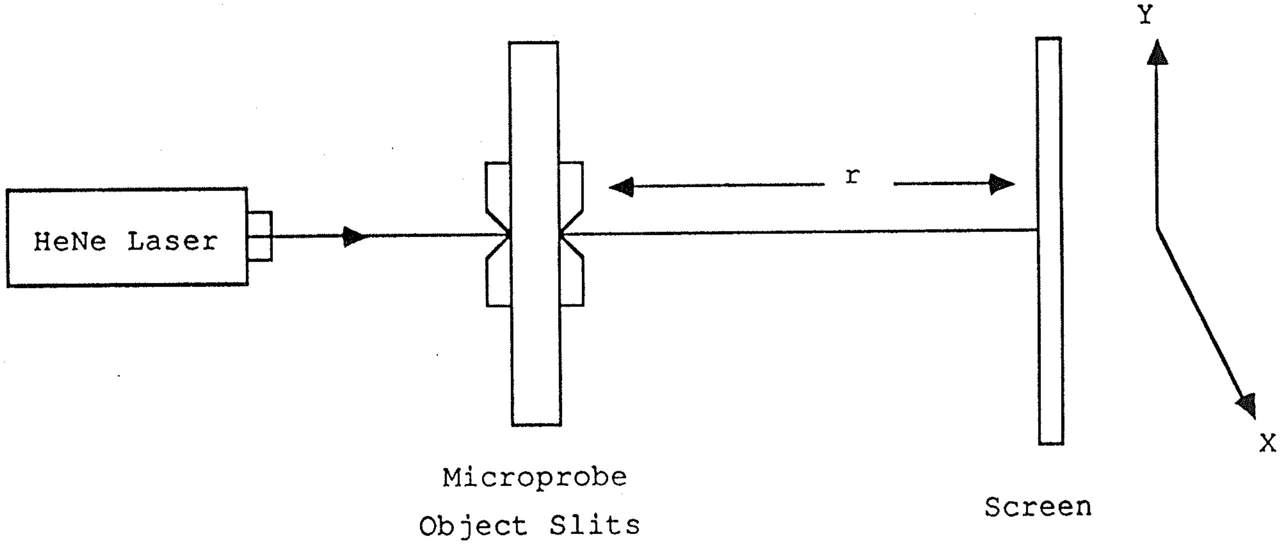

Figure 1.3.2 Experimental setup for calibration of the microprobe object slit.

where a and b are the half dimensions of the object slit. In this case, the MA-HEM object slit was determined to have dimensions of 2a=(72 +/- 2) µm and 2b=(72 +/- 2) µm.

### 1.3.2 The 'Russian quadruplet'

The critical components of the focusing system are the slit used to define the object aperture, and the magnetic lens system used.

The microprobe quadrupole lenses were designed to minimize surface roughness of the pole tips which ensures uniformity of the magnetic field and minimizes parasitic aberrations. Figure 1.3.3 shows the cross sectional geometry of the quadrupole lens used. These microprobe quadrupoles exhibit excellent differential linearity in the central 30 mm of the magnet bore, as shown in Figure 1.3.4.

The magnetic field mapping of the 'Russian quadruplet' was done using a Bell 640 incremental Gaussmeter and a transverse probe. The dimensions of the probe are l=25.4 mm, w=3.7 mm and h=1 mm. A 2 m long plastic tube was designed to hold the probe during the magnetic field measurement. The transverse probe was placed at 1.43 cm from the centre of the magnet bore. The magnetic field was then measured as a

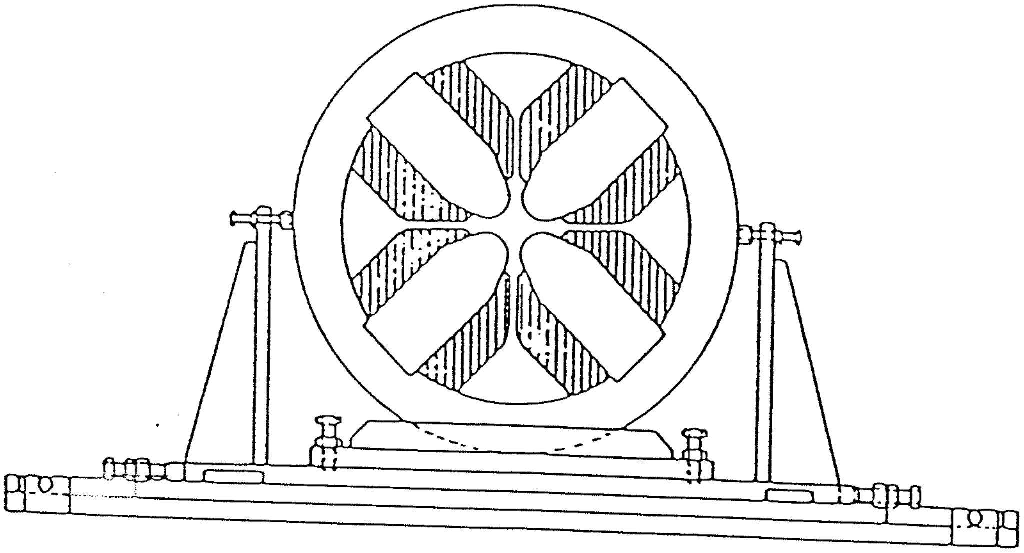

Figure 1.3.3 The cross sectional geometry of the quadrupole lens used.

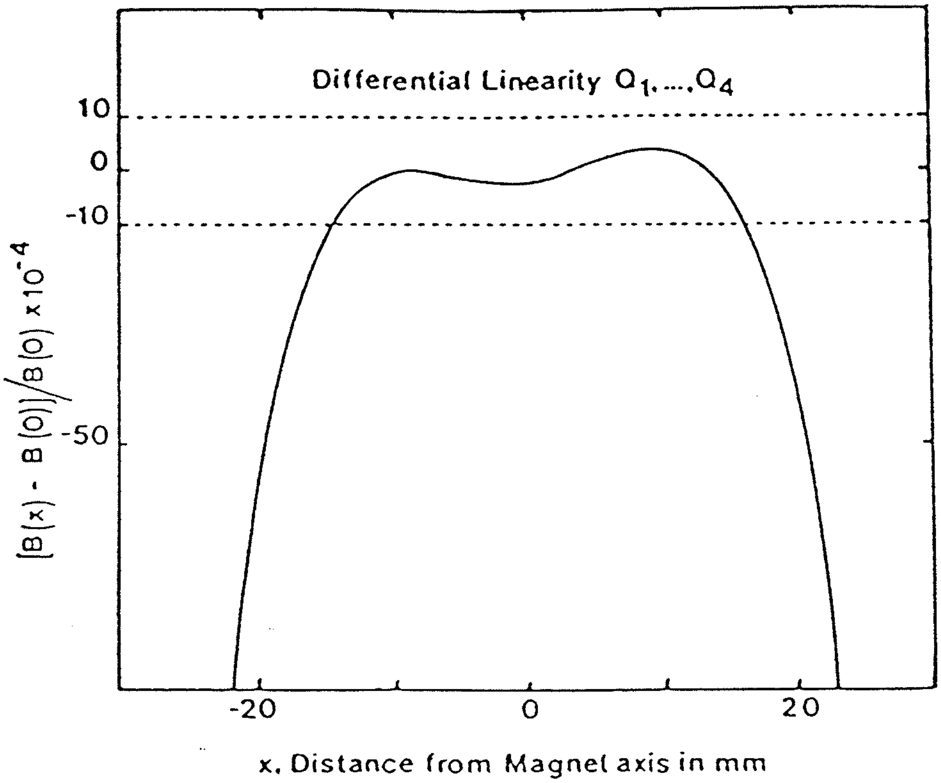

Figure 1.3.4 Differential linearity of microprobe quadrupoles.

function of the current applied to the magnet coils. All the measurements were done in the region where the magnetic field strength is a maximum. Figure 1.3.5(a), (b), (c), (d) show the variation of the field strength with current for all four quadrupole magnets. The relationship between the field strength and current is linear, as expected.

The average B field measured at 100 A for the quadruplet system is (305 +/- 3) mT. The operating condition for the quadrupole requires 599.1 mT at the pole tip for a 100 A excitation current. A simple calculation shows that this requirement is satisfied by the measured value. The uncertainty in the field results from two sources: First the tranverse probe is of finite size. Thus the measured values of the B-field are averaged over the area of the transverse probe; and secondly there is always the possibility of a misalignment of the quadruplet system.

### 1.3.3 Alignment

The slit, quadrupole magnets and target chamber must be located relative to the design axis of the beam from the accelerator. This can be done using conventional surveying techniques involving alignment lasers, telescopes and/or a theodolyte. The Manitoba microprobe system was aligned using a theodolyte. The optical axis of the system is taken to be the path of a particle which passes through the tip of a defining spire placed in the switching magnet, the centre of the object slit and a fiducial point on the microprobe-line aligning wall plate.

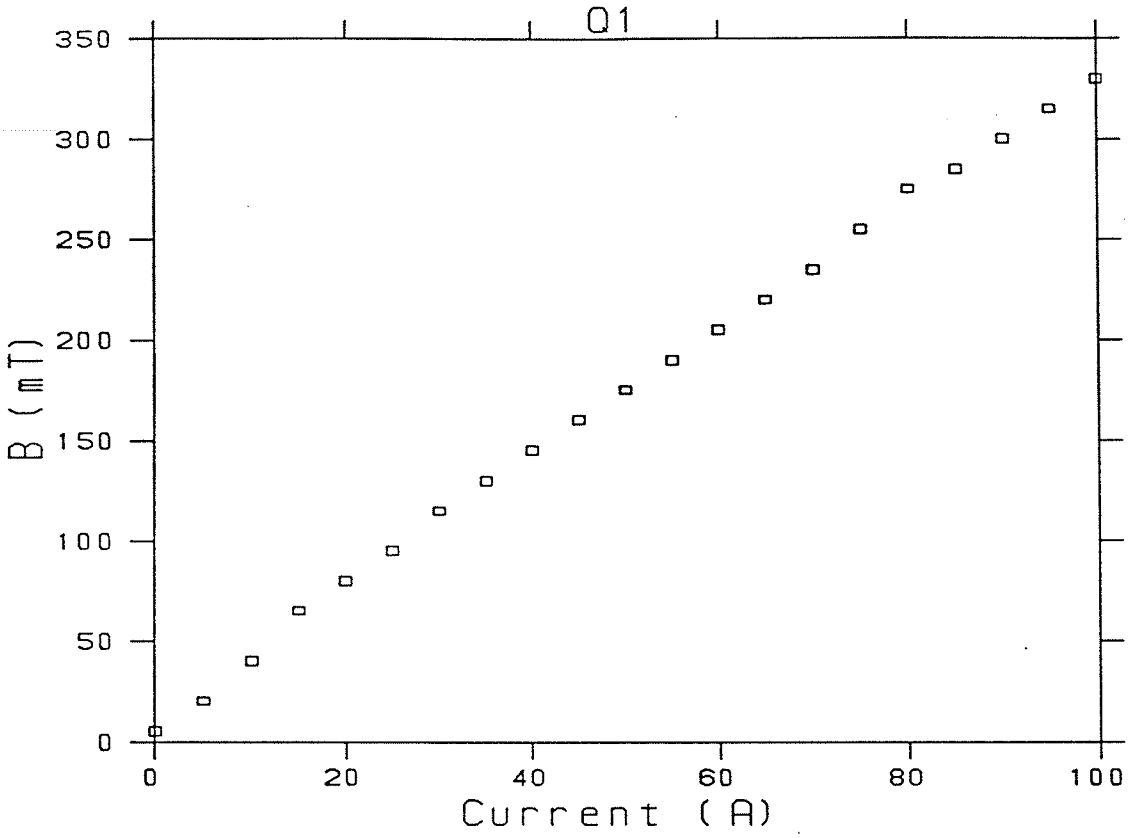

Figure 1.3.5(a) Relationship between field strength and current for $Q_1$.

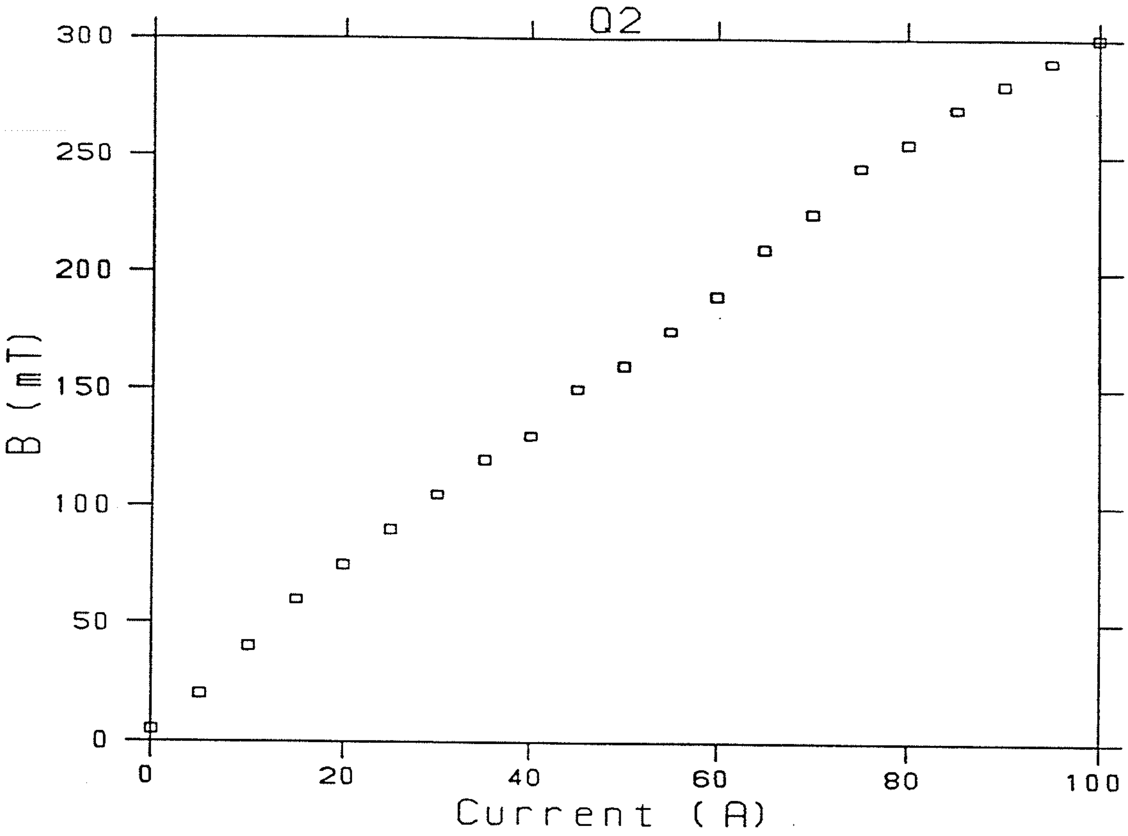

Figure 1.3.5(b) Relationship between field strength and current for $Q_2$.

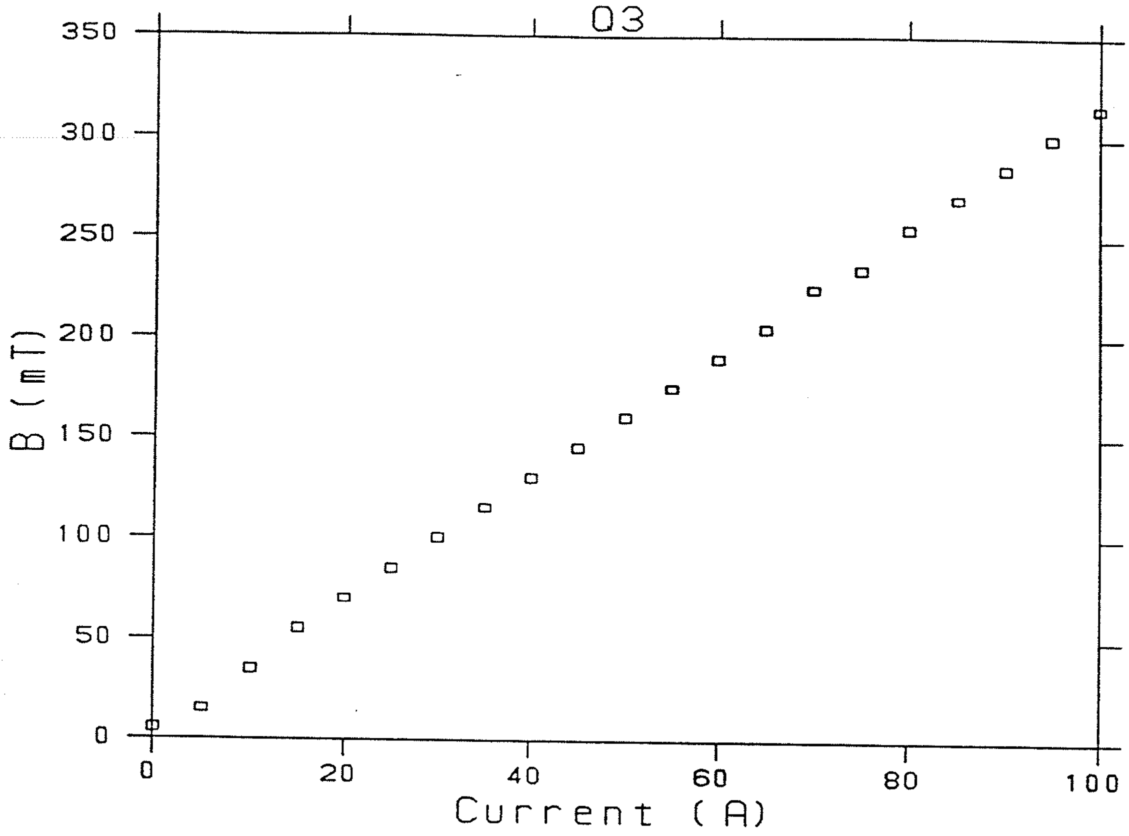

Figure 1.3.5(c) Relationship between field strength and current for $Q_3$.

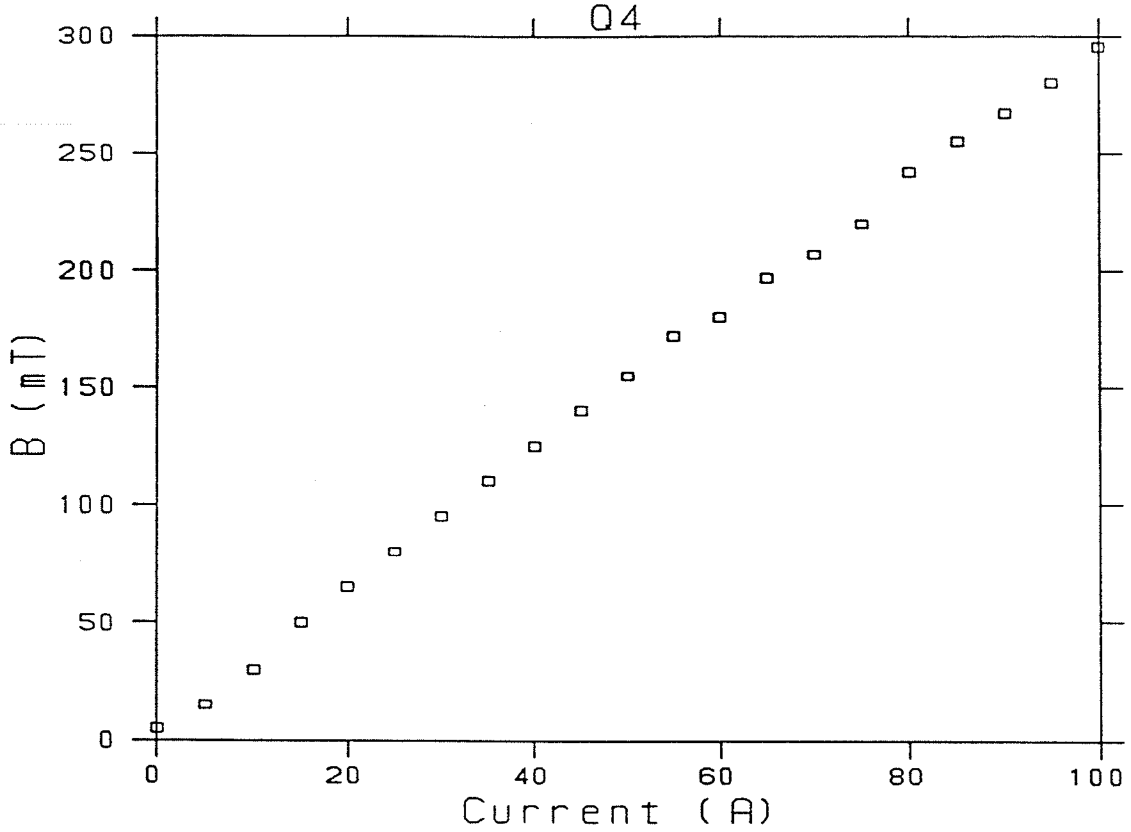

Figure 1.3.5(d) Relationship between field strength and current for $Q_4$.

## 1.4 Preliminary Study

Focusing a 70 µm diameter spot from the object collimation slit to a 10 µm spot at the sample requires a demagnification factor of 7 and the attainment of magnetic field strengths in the 'Russian quadruplet' as mentioned earlier.

Replacing the 70 µm x 70 µm slit with a 3 mm diameter carbon collimator enables a visual examination of the final beam spot using a phosphor screen as the beam passes through the microprobe lens system. A 40 MeV beam spot of roughly 2 mm in diameter was observed visually on the phosphor screen located at the focus of the microprobe. Since previous measurements indicate that the actual beam size is roughly 1/5 the observed size due to the multiple scattering of the proton beam on the phosphor screen, the actual beam spot size observed is then roughly 0.4 mm. This implies that a demagnification factor of 7 is achieved from the 'object' to 'image' for the microprobe focusing system. This is the first experimental verification of a design parameter for MA-HEM [7].

The next task was to install the 70 µm x 70 µm object slit into the microprobe beam line. A wall of concrete blocks was erected between the object slit and quadruplet system to attenuate background radiation coming from the upstream portion of the beam line and arriving at the target stage.

A 125 μm thick lead sheet was then placed at the focus of the microprobe. Using the PIXE technique, an experiment was performed for a run time of 30 min. A standard $^{241}$Am source was used to calibrate the HpGe solid state detector. Figure 1.4.1 shows the effect of a 40 MeV, unfocussed 70 pA microbeam on the lead sheet. Four clearly distinguishable K x-ray lines from the lead were observed. This result confirms the transportation of a microbeam from the object slit to the focal point of the microprobe assembly.

It is useful to obtain a preliminary knowledge of the dimensions of the beam spot prior to subsequent use of the microprobe. A piece of thin mylar was placed at the focus of the microprobe and irradiated with a 40 MeV microbeam for approximately 3 hours. The size of the resultant beam spot was measured to be roughly 100 μm in the vertical direction and 50 μm in the horizontal direction. The final measurements were made using a travelling microscope.

The fact that the spot size measured here is larger than

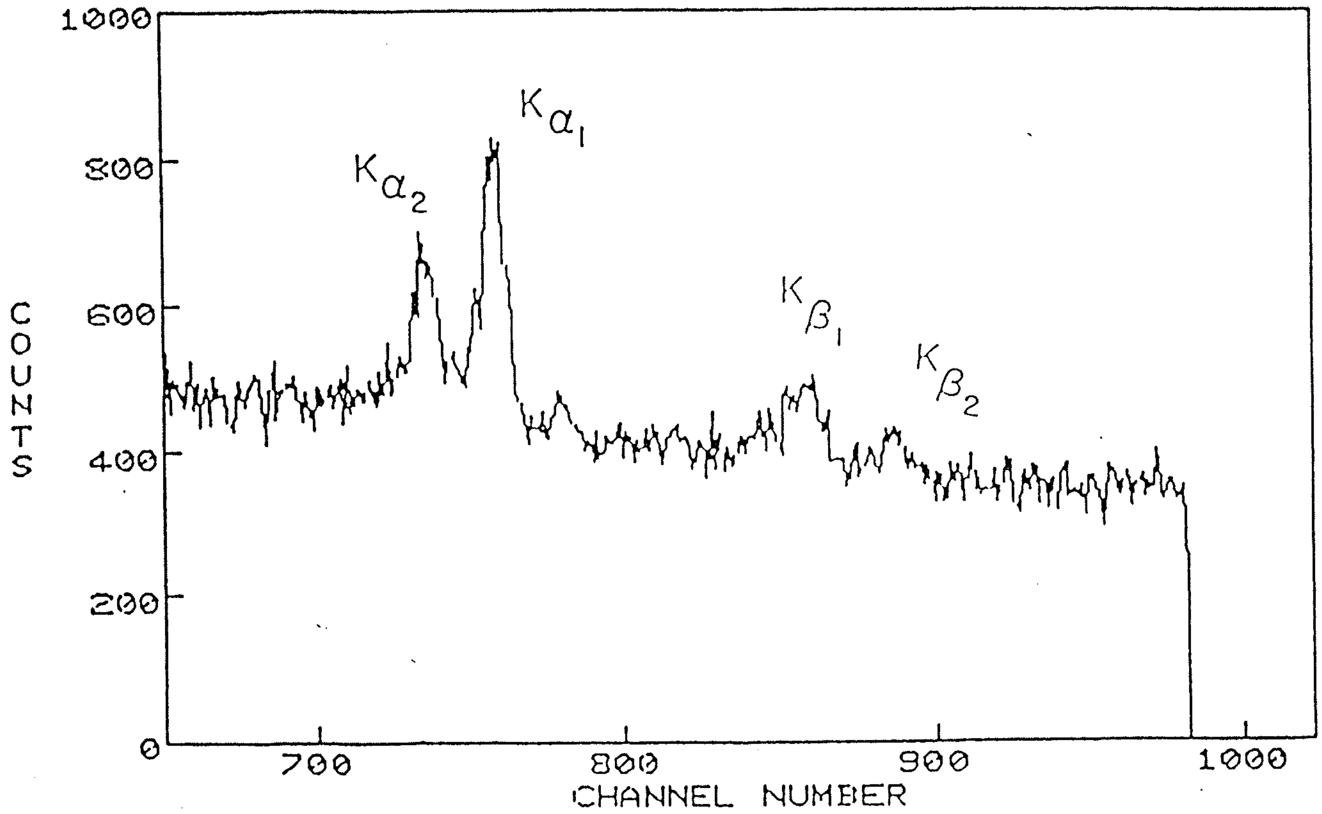

Figure 1.4.1 Raw data from a 125 µm lead target bombarded by an unfocussed 40 MeV, 70 pA proton beam.

the anticipated instantaneous 10 µm dimension is due to the nature of this measurement and to factors involving long term beam stability and mechanical vibration. A granite table and isolation bellows have now been acquired which it is believed will solve this problem. Feedback of current information through use of a downstream split-ionization chamber for example, may be advisable in the future for routine automatic operation. The accurate measurement of the instantaneous spot diameter can however now be made, and details of that technique are given in the paragraphs which follow.

## 1.5 Measurement of the Spot Diameter

### 1.5.1 Introduction

The spot size of a microbeam system is usually determined by sweeping the beam over a sharp edge such as an evaporated strip of metal, a fine wire or the bars of a microscopic mesh [8], and recording the PIXE signal from the metal as a function of the position of the target. The spot size can then be determined from the range of positions over which the signal increases. This process must be repeated with the target moving in the other direction, perpendicular to the first, to obtain the dimensions of the spot in both x- and y- directions. In the early days of low energy proton microprobe development, optical objective lenses were used to magnify the microbeam spot so that its dimensions could be studied by measurement on a projected screen. This method is, however highly expensive and inappropriate for a high energy microbeam.

### 1.5.2 MA-HEM Beam Scanning Stage

The measurement of the dimensions of a high energy proton microbeam is far from simple task. Because of the overall radiation field in the vicinity of the target stage, remote monitoring of the beam and its interaction with matter is essential. A television camera provides a means of monitoring experimental conditions visually. The method chosen for measuring the beam spot of MA-HEM is as follows [9]. A 10 or 20 μm tungsten wire is moved perpendicularly and horizontally across the beam at the focus of the microprobe. Interaction of the microbeam with the tungsten wire results in the production of tungsten K x-rays. These K x-rays are then detected by a HpGe detector and their intensity is recorded as a function of the position of the wire. The dimensions of the beam spot can then be obtained by identifying the full width at half height in the resulting profile [10].

As a means of moving the wire, it was decided that a digitally controlled stepping motor would be most suitable. The schematic layout of the scanning stage is shown in Figure 1.5.1. Simplicity and precision were the reasons for choosing the worm gear coupled to a rack and pinion for the transmission of motion. The tungsten wire is mounted (glued with epoxy) across a 'C' shaped metal frame. This is in turn connected to a rod passing through the target chamber wall by means of a double O-ring seal. The rod is then bolted to the rack.

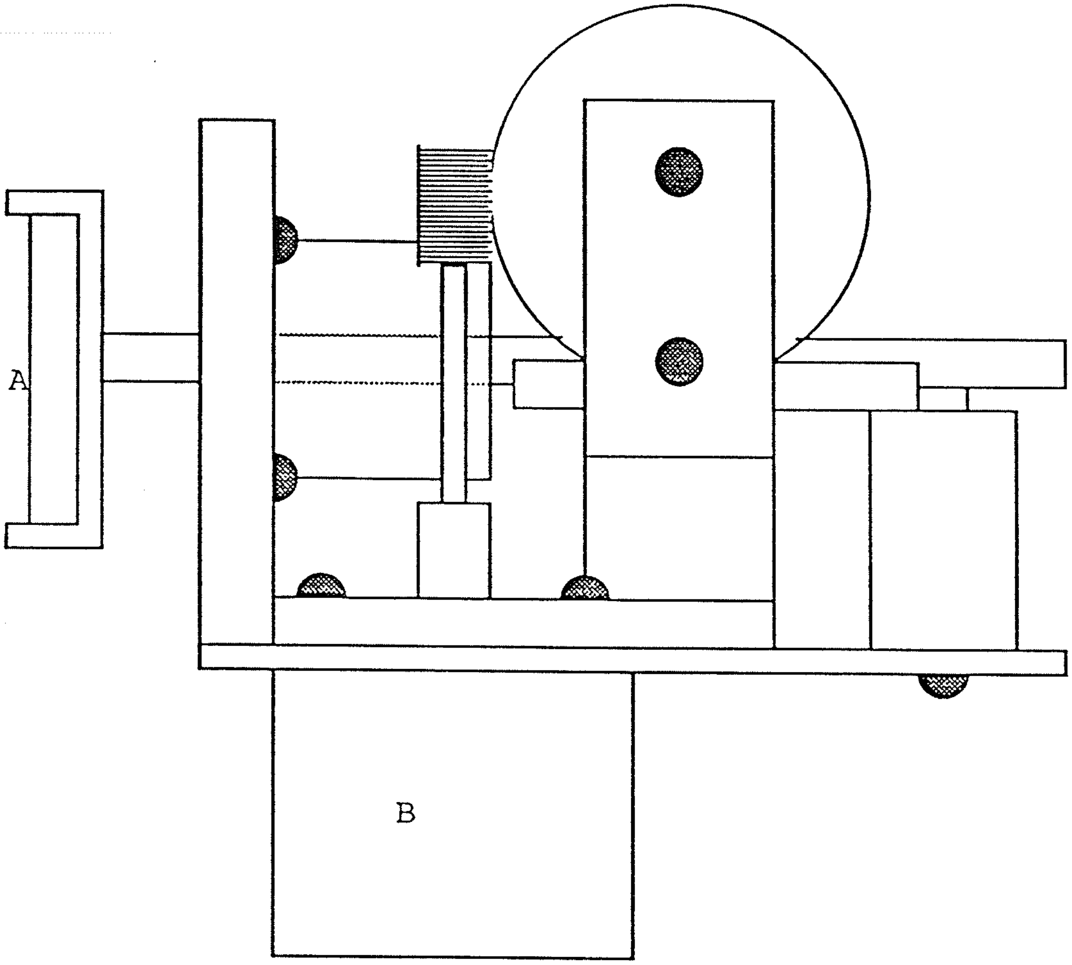

Figure 1.5.1 Schematic diagram of MA-HEM beam scanning stage where A: 10 or 20 µm tungsten wire

B: Stepping Motor.

The target chamber is cylindrical, machined from a aluminum pipe six inches in outer diameter and five inches in inner diameter. Two, one inch wide horizontal slots which allow passage of x-rays, are cut along an arc of the cylinder and covered with the x-ray transparent material, kapton. Both HpGe and SiLi detectors may then be positioned at these two slots, which are $45^{o}$ to the beam axis.

The movement of the stepping motor is controlled remotely by a set of electronic hardware situated in the cyclotron control room. A schematic layout of these pieces of hardware is shown in Figure 1.5.2.

A Chronetics pulser is used to generate a time base for the stepping motor controller. Each pulse causes the MBD to perform a time related function such as pulsing the motor. The function of the LRS3511 ADC is to notify the MBD that a time base pulse has occured. An Input Gate-Output Register, 'IGOR' is used to control both the direction and movement of the motor. The MBD, and thus the VAX has complete control of the stepping motor. The overall scanning system has been completed and is operational.

For every step of the motor, the tungsten wire will move an increment of 0.5 μm. A PIXE experiment will then be

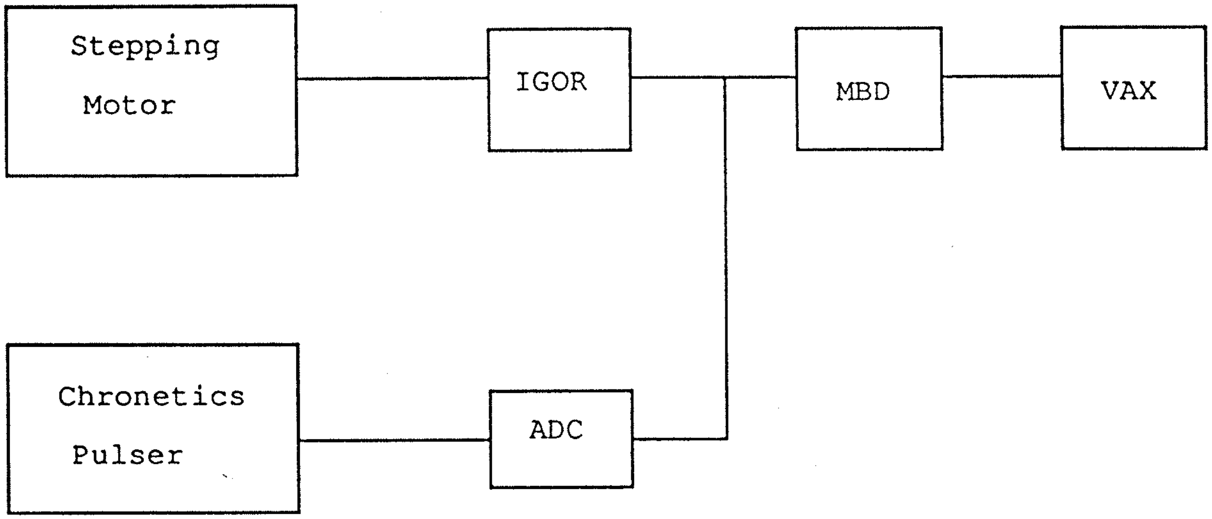

Figure 1.5.2 Schematic drawing of the electronic hardware used to control the scanning stage.

performed at this position and the intensity of the resulting x-rays recorded. This procedure is repeated until a profile is obtained and analysis of this profile will yield the dimensions of the beam.

## 1.6 Future Work

### 1.6.1 Alignment of the 'Russian quadruplet'

Parasitic aberrations of a focusing system are largely due to imperfect alignment of the lens relative to the beam axis. Three common mechanical misalignments of a quadrupole lens are: transverse displacement of the lens, tilting of the lens and rotation of the lens about the beam axis. These misalignments will cause parasitic aberrations which result in degrading the size of the final beam spot [11]. Hence proper alignment of the lens system is required prior to detailed investigation of the beam spot size.

### 1.6.2 Quadrupole Power Supply

To avoid degrading the focus of the final beam spot due to field fluctuations, the power supplies used to excite the magnet coils should have sufficient stability and precision. In practice, the current applied to the magnet coils is required to be stable to the order of 1 part in $10^5$ or better.

The power supply currently used for the outer doublet of the MA-HEM quadruplet has a stability of 1 part in $10^3$, while the supply for the inner doublet has a stability of 1 part in $10^5$. In order to achieve a fine focus of the microbeam, it is required that the existing power supply for the outer doublet be replaced by a high stability constant current supply.

### 1.6.3 Vibration Isolation

It is important to ensure that the target chamber does not move relative to the microbeam during the analysis of the beam spot or samples. The most likely cause of target chamber movement is building and pump vibration transmitted to the target stage through the equipment supports. Any vibrating equipment associated with the target chamber, such as vacuum pumps, needs to be well isolated from the target/magnet system.

As of today, the MA-HEM target stage is not isolated from vibrations. This implies that the results of the preliminary measurement of the beam spot using the thin mylar is not 'vibration free'. Hence the actual beam spot is most probably much smaller than the measured dimensions when vibration is taken into account. To further the study on the nature of the beam spot, it is suggested that the target chamber be isolated from the vibrating equipments with anti

-vibration mountings and flexible connections.

## 1.7 Conclusions

In conclusion, a proton microprobe operating at 40 MeV has been constructed. Preliminary results show good agreement with the design parameters. The performance of the major components of the microprobe and the overall system is as expected. Time and financial contraints have prevented the scanning of the beam spot using the newly designed scanning stage. However, it is expected that the beam spot size is roughly 10-20 μm in diameter when all the necessary improvements to the system, such as those mentioned in the last section, have been completed.

# Chapter Two

## The Role of Cold and Hot Fusion in the Implantation of Palladium and Indium by Deuterons.

## 2.1 Introduction and Motivation

Nuclear fusion is a process involving the combination of two light nuclei to form a heavier nucleus. It is well known that fusion of isotropic hydrogen is an efficient mechanism for energy production. In the case of two deuterium nuclei, in order for the two nuclei to come sufficiently close together to interact, they must first either pass over or tunnel through the Coulomb barrier. For 40 years, it has been believed that such a fusion process is only possible in an environment of temperature in excess of a million degrees.

The Deuterium fusion reaction includes:

$$\mathrm{D} + \mathrm{D} \text{ ------> } {}^{3}\mathrm{He} + n + 3.2\ \mathrm{MeV}$$

$$\mathrm{D} + \mathrm{D} \text{ ------> } \mathrm{T} + p + 4.0\ \mathrm{MeV}$$

$$\mathrm{D} + \mathrm{T} \text{ ------> } {}^{4}\mathrm{He} + n + 17.6\ \mathrm{MeV}$$

$$\mathrm{D} + {}^{3}\mathrm{He} \text{ ----> } {}^{4}\mathrm{He} + p + 18.3\ \mathrm{MeV}$$

The first two reactions indicate that the D-D fusion can follow either of two paths, either producing helium-3 and a neutron or tritium and a proton. Both of these reactions are equally probable. The heavy products of the first two reactions become reactants in the third and fourth reactions. The entire reaction

$$D + D \longrightarrow {}^4He + p + n + \text{energy}$$

results in a net release of energy of 21.5 MeV.

Cold fusion which takes place at room temperature is possible. One mechanism for cold fusion involves replacing the electron in a $D_2^+$ molecule by a negative muon [12]. The more massive particle reduces the separation between the two deuterium nuclei by a factor 200, and consequently increases the neutron tunnelling probability by about 85 orders of magnitude over that expected for a normal molecule.

Another approach to the phenomenon of cold fusion has recently been studied in some detail by Fleischman and Pons [13] and Jones et al. [14]. Both groups employed a conventional electrolytic cell with a platinum anode surrounding a palladium cathode. The electrolyte of the cell consists of $D_2O$ (99.5% enriched) made conducting by the addition of LiOD. Fleischman and Pons observed an abnormal energy release and neutron emissions from the positive palladium electrode; however, the Jones's group observed only the neutron emissions and no major energy release. As of today, more than fifty laboratories around the world have tried to duplicate the experiment using a similar arrangement. Unfortunately, most do not confirm the reported results. Recent calculations [15] based on neutron tunnelling suggest that the rate for D-D cold fusion is roughly 3 x $10^{-64}$ per deuteron pair per second. This calculation has not yet been confirmed experimentally.

While neither the complete experimental facts of the situation nor an adequate theoretical model for such processes are currently available, it seems that the formation of high concentrations of deuterium nuclei in the palladium metal could be a prerequisite for the cold fusion process. At the University of Manitoba Accelerator Centre, several experiments involving the direct implantation of deuterium nuclei into metal surfaces were performed, based on the above assumption. The motivation was to investigate the results of the Fleischman and Pons electrolysis experiment in a similar non-equilibrium situation that did not involve heavy water ($D_2O$) as an intermediate material.

## 2.2 Ion Implantation with the Narodny Ion Accelerator

The process of implantation of 60 keV $D_2^+$ and $D^+$ ions into the palladium was carried out using the Narodny Ion Accelerator (NIA). The schematic diagram of the NIA is shown in Figure 2.2.1. The ion source is a duoplasmatron type, capable of producing positive ions of the feed gas which may then be accelerated to energies between 30 and 120 keV. Because the beam is created by an electrical discharge, both $D_2^+$ and $D^+$ (with estimated ratio $D_2^+:D^+ = 2:1$) ions populate the plasma and are extracted from the ion source and accelerated by a 60 kV potential difference. Upon hitting the target, a $D_2^+$ ion dissociates into two 30 keV $D^+$ ions.

Three different samples [(Pd-In), In, (Pd-C-In)] were mounted on the target holder and then subjected to bombardment by the $D_2^+$ and $D^+$ ions for an period of time. In each case, the implanted surface was that of the first element listed, namely Pd, In and Pd.